Experimental Evaluation and Numerical Simulation of RCS of Target using GBL and GBS

Helmi Ghanmi, Ali Khenchaf, Philippe Pouliguen

Experimental Evaluation and Numerical Simulation of RCS of Target using GBL and GBS

GHANMI Helmi
Lab-STICC UMR CNRS 6285
ENSTA Bretagne
Brest, France
helmi.ghanmi@ensta-bretagne.org

KHENCHAF Ali
Lab-STICC UMR CNRS 6285
ENSTA Bretagne
Brest, France
ali.khenchaf@ensta-bretagne.fr

POULIGUEN Philippe
French General Directorate for Armament
Paris, France
Philippe.Pouliguen@intradef.gouv.fr

***Abstract*— In this work, two Gaussian Beam (GB) techniques were presented for investigating the radar cross section (RCS) of a cylinder with and without an aperture. Therefore, we have carried out experimental measurement of RCS of different PEC targets in the anechoic chamber. These measurements were used to validate the numerical results obtained using the GB approaches which are: Gaussian Beam Summation (GBS) and Gaussian Beam Launching (GBL). In the numerical simulation, the used GB techniques are firstly combined with the asymptotic Physical Theory of Diffraction (PTD) method. After that, the RCS results are evaluated with the Method of Moment (MoM) and also with the experimental measurements.**

Keywords—Radar Cross Section (RCS), Radar Target, Gaussian Beam (GB), Gaussian Beam Summation (GBS), Gaussian Beam Launching (GBL), Physical Optic (PO), Physical Theory of Diffraction (PTD), Method of Moment (MoM),

I. INTRODUCTION

The modeling of electromagnetic scattering and Radar Cross Section (RCS) of the different targets presents a significant role in the radar object identification. Therefore, several numerical methods have been developed to model electromagnetic scattered fields by canonical and complex targets. The asymptotic methods such as Physical Optic (PO), Physical Theory of Diffraction (PTD), Geometrical Optics (GO), Geometrical Theory of Diffraction (GTD) and Equivalents Current Method (ECM) are considered as approximations of high frequencies [1], [2], [3]. The advantage of asymptotic methods lies to the speed of calculation time (take into account the complexity of the object). However, the critical points of some asymptotic methods are related to the transaction between highlighted and shadowed region and the caustic problem. To overcome this problem, others asymptotic techniques based on GB have been developed. Among them, Gaussian Beam Summation (GBS) and Gaussian Beam Launching (GBL) methods [4]-[13]. These (GBS, GBL) methods are used in this work to estimate the RCS of a modified canonical target.

The GBL technique has been introduced and applied in the research published by H. T. Chou [4]. In this method, when a radar target is illuminated by a GB, is firstly necessary to decompose the radiated field into a plane wave spectrum then summing the contribution of the radiations of all the beams interacting with the target.

The GBS as an asymptotic approach for computing high-frequency wave fields was developed by V. Cerveny and M.M. Popov [9]-[12]. The summation of GB allows solving some limitations of the asymptotic ray methods such as the problems related to the evaluation of wave field in singular areas and the resolution of the caustics problem [4]-[13].

In the works of P. O. Leye et al [6], the GBS and GBL methods were applied in the simulation of RCS of a metallic flat plate. These methods are also compared only with PO and MoM methods. However, this paper presents a new investigation on the Gaussian techniques GBS and GBL. Moreover, we will extend the application of the Gaussian techniques (GBS, GBL) in the estimation of radiated field by various targets (cylinder with an aperture, shell cylinder). In addition, the obtained RCS results have been compared with the others numerical methods and also with the experimental measurements realized in an anechoic chamber.

This paper is organized as follows: Section II shows the general mathematical formulation of the GBL and GBS methods. Section III describes the measuring devices. Section IV, illustrates the numerical and experimental results of RSC of different radar targets (hollow cylinder with an aperture, shell cylinder). The final section presents the conclusion and the future works.

II. FORMULATION OF THE GAUSSIAN TECHNIQUES GBL AND GBS

A. Theoretical formulation of GBL technique

In [4] and [5], the GBL technique has been used in the analysis of fields radiated by parabolic, non-parabolic reflector antennas and quasi-optical multi-reflector systems. In the present work, the GBL was applied in the calculation of the RCS of canonical and modified targets.

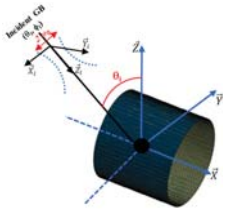

Fig. 1. Geometric configuration of a cylinder illuminated by incident Gaussian Beam (GB), width ($2\omega_0$).

Consider a target (plate, disk, cylinder,…) illuminated by a Gaussian beam as shown in Fig.1, the GBL method is applied to calculate the radiation integral of the fields scattered by the target. For the considered Gaussian beam, the incident magnetic field is given by the following form [4], [6]:

$$H_i(r_i) = H_i(0)\sqrt{\frac{\rho_i + jb_i}{z_i + \rho_i + jb_i}}.\exp\left(-jk.\left(z_i + \frac{x_i^2 + y_i^2}{z_i + \rho_i + jb_i}\right)\right) \quad (1)$$

In (1), the distance between the waist the incident GB and each point on the illuminated surface is indicated by the parameter ρ_i, the position vector in the GB is defined by and $b_i = k.\omega_0^2/2$, where k, ω_0 are the wave number and the half beam-width respectively. The electric fields scattered from the target surface (Σ) illuminated by the incident field is given by the integration of the incident GB on the reflector surface (PO integral). This integral is written by (2):

$$E(r) = \frac{j.k}{4.\pi}\iint_{\Sigma}\left[\frac{Z_0}{\sqrt{\varepsilon_r}}.R\times R\times\left(e_z\times H_i(r_i)\right)\right]\frac{\exp(-j.k.R)}{R}.ds \quad (2)$$

Finally, by using equation (1) in (2) and determining the integral, we can calculate the scattered field by applying GBL formulation as in [4], [6].

B. Theoretical formulation of GBS technique

The physical principle of GBS technique consists in a compatible step assembly. Consider a homogeneous and isotropic medium and an electromagnetic wave propagating in this medium which is acting excited by a point source. In the GBS method, the total field at the receiver is a sum of the contributions of all the beams passing in the vicinity of the receiver (which is the same case for each observation point). For each considered ray, we determine a Gaussian beam propagating along the ray. Then we sum the contribution of each Gaussian beam to the receiver overall rays [11], [12] .

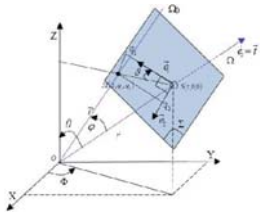

Fig. 2. Geometric configuration and coordinate parameters for GBS formulation.

Fig. 2 shows the ray-centered coordinate system *(s, q_1, q_2)* used to formulate (3) of the Gaussian beam amplitude u*(s, q_1, q_2, t)*. This coordinate system is connected to any selected Ω radius. In addition to the geometric parameters, others assumptions are also used to establish the theoretical equation of GBS. In fact, we start by considering a homogeneous and isotropic medium an electromagnetic wave propagating (with a propagation velocity v) in this medium which is being excited by a point source. Then, we suppose that some wave process is described by the Helmholtz's wave equation and the point source is positioned in the origin. After, we solve the Helmholtz's equation in the neighborhood of rays. As function of the local coordinates and at the receiver point, the solution of the Helmholtz equation as a solitary GB is given by (3) [12], [6]:

$$\begin{cases} u(s,q_1,q_2,t) = \left(\dfrac{v}{\det[Q]}\right)^{\frac{1}{2}}\cdot\exp\left\{-j\omega\left[t-\tau(s)-\dfrac{1}{2}\left(q^T\cdot P\cdot Q^{-1}\cdot q\right)\right]\right\} \\ \tau(s) = \displaystyle\int_s \frac{ds}{v} \end{cases} \quad (3)$$

In (3), v represents the propagation velocity; q^T is the transpose of the q vector; the travel time from the source along the designated ray is represented by $\tau(s)$. The parameters Q and P are two-by-two matrix named "dynamic quantities" which are related by the "Dynamic Ray Tracing" (DRT) [10], [13]. These two parameters (Q and P) will be used in (3) to determine the final equation of the Gaussian beam amplitude u.

In the case of homogenous media, by using the Q and P values in (1), we return to the representation of the amplitude u of the Gaussian beam in 3D [10], [6]:

$$u(s,q_1,q_2) = \frac{c^{\frac{3}{2}}}{\omega.\omega_0^2 + j.(s-s_0)}.\exp\left(j\omega\left(\tau(s) + \frac{1}{2}\frac{(q_1^2+q_2^2)}{c.\left(-j\frac{\omega.\omega_0^2}{c}.+(s-s_0)\right)}\right)\right) \quad (4)$$

Finally, to calculate the full amplitude (u^{GBS}) at the receiver we must use an integral formulation as shown in (5). This integral will be calculated on all Gaussian beams described by their characteristic angle (called takeoff angle φ) from the source:

$$u^{GBS} = \int_{\gamma}\Phi_{\varphi}.u_{\varphi}(s,q_1,q_2).d\gamma \quad (5)$$

The integral function in (5) is the product of three terms. The first term denoted Φ_φ is the complex weight function which may differ from ray to ray, however, remains constant in each considered ray. The second term is the function $u_\varphi(s, q_1, q_2)$ is the Gaussian beam related to the ray given by (4). Finally, the third term $d\gamma$ is expressed according to angle φ by the equation ($2\pi.sin(\varphi).d\varphi$). The choice of the integration domain γ is related to the function of the Gaussian beam $u_\varphi(s, q_1, q_2)$ and to the central ray. In fact, the domain γ is fixed on the central ray and delimits the Gaussian beams propagating in the neighbor of the central ray. On the other hand, the contribution of the Gaussian beams $u_\varphi(s, q_1, q_2)$ is conditioned by the fact that outside the γ domain do not contribute effectively to the wave field.

The GBS integral (5), may be evaluated asymptotically using the saddle-point method. Thus, this result must coincide with the above ray asymptotic solution in regular region. This integral of GBS is simulated numerically and quadratically by a regular increment denoted $\Delta\varphi_k$ (6).

$$u^{GBS}(M) = 2.\pi.\sum_{k=1}^{N}\Phi_{\varphi k}.u_{\varphi k}.\sin(\varphi_k).\Delta\varphi_k \quad (6)$$

The integral formulation (2) and (5) of GBS and GBL techniques, respectively, can be used to calculate the scattered field in the case where the radar target is described by a set of triangular facets. In fact, to compute the scattered fields, the target geometries are modeled by triangular facets. The centers of these triangles become the positions of the bright points (as displayed in Fig. 3). Then, after the visibility test, the scattering field integral from each visible triangular is calculated by GBS and GBL techniques. On the other hand, the work in [6], [7] show that when the diffraction contributions are accounted, the GBS+GTD method gives an accurate qualitative representation of the RCS variation for all observation angles. Therefore, to consider the edge diffraction contribution, we have chosen to combine the GBS and GBL with the physical theory of diffraction (PTD) method [2]. In fact, PTD method is used to compute a diffraction part for each ray that hits the target surface in the vicinity of an edge and is calculated in the complex weight function in the integral (5).

Fig. 3. The mesh representation of a hollow cylinder with an aperture.

III. Description of the Measuring Devices

The evaluations of the numerical simulation results with experimental measurements have been done in anechoic chamber (8m × 5m × 5m) at the Lab-STICC, ENSTA Bretagne (Fig. 4). The characteristics of various measurements components system are: All walls are covered with absorbent material. A computer controls the Vectorial Network Analyzer (Anritsu 37347D) which operates in the frequency range from 40MHz to 20GHz and the positioning system. The NEWPORT positioning system with an angular resolution equal to 0.01° and an angle vary between -90° and 90°. Finally, an elevation motor is used for the modification of the height position of the target.

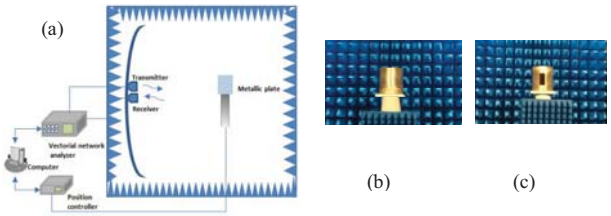

Fig. 4. (a) Description of the experimental setup, (b) Metallic cylinder, (c) Metallic cylinder with an aperture.

IV. Numerical and Experimental Results: Investigation on RCS of a Hollow Cylinder with an Aperture

In this section, we present the results of RCS of a hollow circular cylinder (which is not covered at the end) with and without an aperture. As illustrated in Fig. 5, in the geometrical scattering configuration of the target, the incident angle θ_i equal 90° and the azimuth scattering angle φ_i vary from -90° to 90°. It is supposed that rotation is around to z-axis. This geometrical configuration allows giving the possibility to find the effect of the rectangular aperture at the center of the cylinder on the RCS variation.

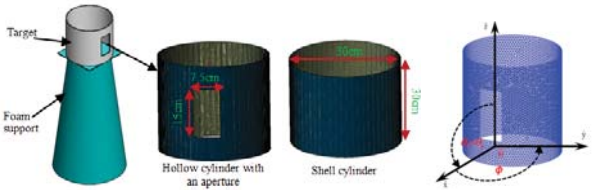

Fig. 5. Dimension and geometric configuration (monostatic) of a hollow circular right cylinder with an aperture: r = 15cm and h = 30cm, aperture (15 × 7.5) cm.

Fig. 6 and Fig. 7 compare the measured and simulated monostatic RCS of a circular cylinder without and with an aperture respectively. The simulations are obtained by using the MoM method, the GBS and GBL techniques which are combined with PTD method (GBS+PTD, GBL+PTD).

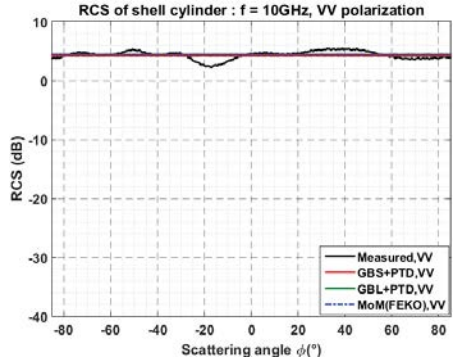

Fig. 6. Measured and simulated RCS of a circular cylinder: 10GHz, *vv*.

In Fig. 6, it is observed that in the case of a circular shell cylinder, the RCS simulated using (GBS+PTD, GBL+PTD and MoM) is constant (4.5 dB) over the entire range of the scattering angle. This RCS curve is representative for the cylinder shape observed in the geometrical configuration presented in Fig. 5.

In the case of a hollow circular cylinder with an aperture (Fig. 7 (a)), we can see that the curves of measured RCS and those simulated using GBS+PTD, GBL+PTD and MoM have the same general shape and are close in the scattering angular range outside the specular direction. However, it is observed a peak at 0° corresponding to simulated values of -2.3 dB (GBS+PTD), -4 dB (GBL+PTD) -10 dB (MoM) and measured value of -13 dB. This peak decreases and reaches a minimum measured value of -16 dB, and a minimum values of {-17 dB (MoM), -16dB (Exp), -6 dB (GBL+PTD), -4 dB (GBS+PTD)} at the scattering angle of 2° and 4° respectively. These preliminary results show that the curves simulated using GBL+PTD are closer to the MoM method and the measurements than those obtained using GBS+PTD.

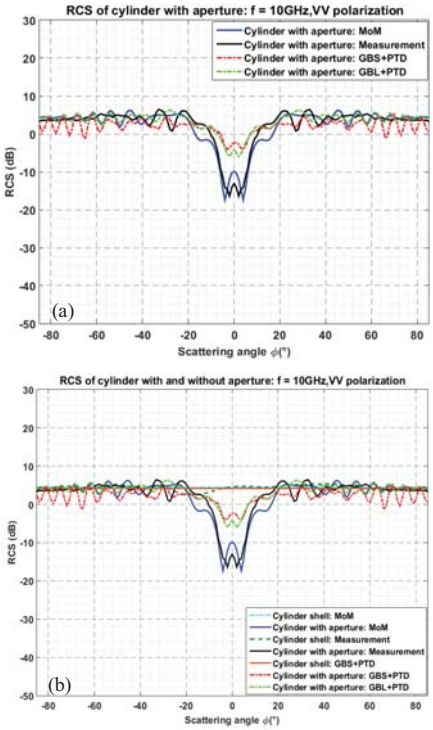

Fig. 7. (a)Measured and simulated RCS of a hollow circular cylinder with an aperture, (b) RCS of a cylinder with and without an aperture.

The deviation between the RCS simulated using Gaussian model (GBS+PTD) and those realized by the MoM method and experimental data is explained by the fact that the Gaussian techniques GBS and GBL consider only a part of multiple interactions due to the presence of the rectangular aperture. These preliminary study results will be used in our future work as a basis for the development and extension of the validity region of the GBS and GBL techniques.

In addition, the comparison between the RCS (measured and simulated) of a cylinder with and without an aperture is illustrated in Fig. 7 (b). From this comparison, we can see that the presence of the aperture reduce the values of the RCS particularly in the scattering angle range from 0° to 20°. This decreasing of RCS value may be due to the multiple interaction phenomenon caused by the rectangular cavity. The other phenomenon caused by the presence of the aperture is appeared on the RCS curves at the scattering angles 20 ° and 30 ° where we observe a curve peaks which due to the edge diffraction of the aperture.

To obtain more information about the impact of the rectangular aperture on the scattered field, we have modeled the normalized RCS (NRCS) of a PEC cylinder (with and without aperture) in bistatic configuration. Fig. 8 illustrates the NRCS of a shell cylinder (b) and a cylinder with aperture (c) simulated as function of the scattering angles (θ_s, ϕ_s) and for one value of incident angles (θ_i, ϕ_i). These simulations have been done using the MoM method in FEKO software. The maximum difference between the NRCS appears in the range ϕ_s angle from 60° to 120° as Fig. 8 displayed.

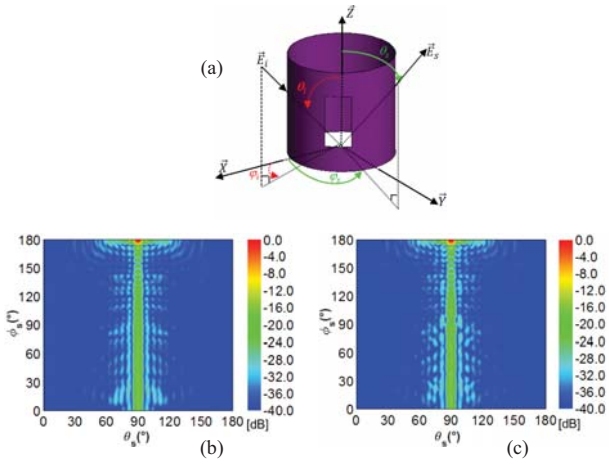

Fig. 8. (a) Geometrical parameters of the bistatic configuration, Normalized RCS of a shell metallic cylinder (b), and a hollow metallic cylinder with rectangular aperture (c) observed in bistatic configuration: $\theta_i = 90°$, $\phi_i = 0°$, $\theta_s = \phi_s = [0:180°]$, f = 10GHz, MoM (FEKO).

These results of investigation will be used as a base of development of GBS and GBL methods for the bistatic case (which is our current work).

V. Conclusion and Future Work

In this paper, investigations and evaluations of the Gaussian techniques (GBS, GBL) were presented. For this, the theoretical formulation of GBL and GBS were established, and experimental measurements of RCS of different targets in anechoic chamber have been done.

In the numerical simulations, the RCS of a cylinder with aperture and a shell cylinder is simulated using GBS+PTD, GBL+PTD and MoM methods. The obtained numerical results are also compared with the experimental measurement. This comparison demonstrated that the Gaussian techniques (GBS, GBL) represent well the field variation of the canonical target (shell cylinder). However, for the case of a hollow cylinder with an aperture, we have found a visible decrease in RCS values is observed in the normal incidence range which is due to the multiple interaction caused by the presence of the aperture. Nevertheless, the results using GBL+PTD are closer to the MoM method and the measurements than those realized using GBS+PTD. The development of the GBS and GBL methods by taking into account the full multiple interactions contribution as in the case of a hollow cylinder with an aperture observed in bistatic case is one of the perspectives of our work.

Acknowledgment

The authors wish to thank the DGA (Direction Générale de l'Armement, France)-MRIS for its support of the SOFAGEMM project, where this work is in Progress.

References

[1] P. Pouliguen, L. Lucas, F. Muller, S. Quete and C. Terret, "Calculation and analysis of electromagnetic scattering by helicopter rotating blades," IEEE Trans. Ant. Prop, vol. 50, no. 10, pp. 1396-1408, 2002.

[2] F. Weinmann, "Ray tracing with PO/PTD for RCS modeling of large complex objects," IEEE Trans. Ant. Prop, vol. 54, no. 6, 2006.

[3] P. H. Pathak, G. Carluccio and M. Albani, "The Uniform Geometrical Theory of Diffraction and Some of Its Applications," IEEE Ant. Prop. Mag, vol. 55, no. 4, pp. 41-69, Aug. 2013.

[4] H. T. Chou, P. Pathak and R. J. Burkholder, "Novel Gaussian Beam Method for the Rapid Analysis of Large Reflector Antennas," IEEE Trans. Ant. Prop, vol. 49, no.16, pp. 880-893, 2001.

[5] C. Rieckmann, M. R. Rayner, C. G. Parini, D. H. Martin, and R. S. Donnan, "Novel modular approach based on Gaussian beam diffraction for analysing quasi-optical multi-reflector antennas,"IEE Proc.,Microw., Antennas Propag., vol. 149, no. 3, pp. 160–167, 2002.

[6] P.O. Leye, A. Khenchaf, and P. Pouliguen, "The Gaussian Beam Summation and the Gaussian Launching Methods in Scattering Problem," Journal of Electromagnetic Analysis and Applications, vol. 8, pp.219-225, 2016.

[7] H. Ghanmi, A. Khenchaf, P. Pouliguen and P. O. Leye, "Study of RCS of complex target: Experimental measurements and Gaussian beam summation method," IEEE CAMA Conference, Tsukuba, pp. 196-199, 2017.

[8] M. Katsav and E. Heyman, "Gaussian Beam Summation Representation of Beam Diffraction by an Impedance Wedge: A 3D Electromagnetic Formulation within the Physical Optics Approximation," IEEE Trans. Antennas Propagation, vol. 60, no. 12, pp. 5843-5858, 2012.

[9] V. Červený, "Seismic Ray Theory," Cambridge: Cambridge University Press, 2001.

[10] V. Červený, "Summation of paraxial Gaussian beams and of paraxial ray approximations in inhomogeneous anisotropic layered structures," In Seismic waves in Complex 3-D Structures, no. 10, pp. 121–159, 2000.

[11] V. Červený, "Computation of wave field in homogeneous media," Geophys. J. R. astr. Soc., vol. 70, pp. 109-128, 1982.

[12] M. M. Popov, "New method of computation of wave fields in high frequency approximation", Mathematical problems in the theory of wave propagation. J. Soviet Math., vol.20, no.1, pp. 1869–1882, 1982.

[13] B. S. White, A. Norris, A. Bayliss and R. Burridge, "Some remarks on the Gaussian beam summation method," Geophysical Journal of the Royal Astronomical Society, vol. 89, pp. 579-636, 1987.